

We are IntechOpen, the world's leading publisher of Open Access books Built by scientists, for scientists

5,000

Open access books available

125,000

International authors and editors

140M

Downloads

Our authors are among the

154

Countries delivered to

TOP 1%

most cited scientists

12.2%

Contributors from top 500 universities



WEB OF SCIENCE™

Selection of our books indexed in the Book Citation Index
in Web of Science™ Core Collection (BKCI)

Interested in publishing with us?
Contact book.department@intechopen.com

Numbers displayed above are based on latest data collected.
For more information visit www.intechopen.com



Mammalian Cell Viability Methods in 3D Scaffolds for Tissue Engineering

Benjamin Gantenbein, Andreas S. Croft and Marie Larraillet

Abstract

Modern methods have evolved in tissue engineering to evaluate cell viability (CV) in 3D scaffolds and tissues. These involve either the usage of 3D confocal laser microscopy of live or fixed tissues, or separation of cells from the tissue, either live or fixed, and then their analysis by flow cytometry. Generally, working with live cells has the disadvantage that all the scanning needs to be completed immediately at the end of an experiment. Two different approaches can be distinguished: staining intact cell membranes and staining fixed cells. The entire cytoplasm is stained with amine-reactive dyes (ARDs), these use the principle of dead cell exclusion. Here, we list and compare live-cell versus fixed-cells fluorescence-based methods and also show their limitations, especially when working with autofluorescent or cross-linking materials like silk or genipin-reinforced hydrogels. Microscopic techniques have the advantage over flow cytometry-based methods in that these provide the spatial distribution and morphology of the cells. Calcein AM combined with ethidium-homodimer works for most 3D constructs, where no strong fluorescent background is found on the tissue or scaffold. Frequently, however, concentrations and incubation times need to be adjusted for a specific tissue to ensure diffusion of dyes and optimise emittance for detection.

Keywords: live/dead staining, 3D scaffold, hydrogels, confocal laser scanning, calcein AM, ethidium homodimer-1, cell tracking, mammalian cells, amine-reactive dyes (ARDs), microscope, fixed cell staining, glycosaminoglycan-rich tissues, fibrin, silk, genipin

1. Introduction

1.1 The need for 3D culture models in tissue engineering

There are several areas of applied research where the importance for ex vivo 3D culture models is crucial, especially if 3D organ culture models are to be established using perfusion or non-perfusion characteristics or even under static culture conditions. These concepts apply to all research areas involving organs and tissues in culture. As the authors of this chapter are active in the field of musculoskeletal research, examples will be illustrated using connective tissues or cells isolated from bone and joints. These fields often focus on joint-derived tissues that cause clinical problems for healing such as (i) anterior cruciate ligament

(ACL) [1–3], (ii) cartilage scaffold engineering [4–7], (iii) intervertebral disc (IVD) regeneration [8–10] and (iv) bone regeneration [11–15]. We demonstrate a subset of fluorescent staining and methods to stain cells from bone and joint-derived tissues: that is, staining mesenchymal stromal cells, chondrocytes and IVD cells in native tissue or in 3D hydrogel-like scaffolds such as fibrin [16], polyethylene glycol (PEG) [17], and also cells on solid materials such as silk [18]. In all of these fields, bioreactor models have been developed to better understand the mechanism of mechanical loading on these tissues. However, the combination of novel smart biomaterials can also be studied together or in direct contact with the organ of interest under more realistic conditions [10, 19–21]. More generally speaking, as the aim is to develop clinically relevant models considering the integrity of tissue and organ explants, judging cell viability (CV) becomes a major issue that needs to be assessed [22]. CV is also the main read-out for new biomaterials and scaffolds to be tested for tissue engineering (TE) and cell therapy applications. Of course, there are other parameters quantified such as DNA content, mitochondrial activity [23, 24] and cell apoptosis [25, 26]. However, in this book chapter, we would like to emphasise CV as a key parameter and summarise the currently most applied methods to stain and visualise living and dead cells. Furthermore, we provide a link of an automated cell counting macro for the integration of ImageJ, a free microscope imaging processing platform to quantify CV [27]. At the end, we would like to present some examples using 3D automated macros for high-throughput screening. The decision whether to analyse cells in a living or dead state has to be made relatively early in the work flow (**Figure 1**). Most fluorescent dyes that are introduced here are commercially available as kits (**Table 1**) [4, 28–31]. However, as many of the patents have expired, most

The two different principles of staining cells from Tissues/Scaffolds

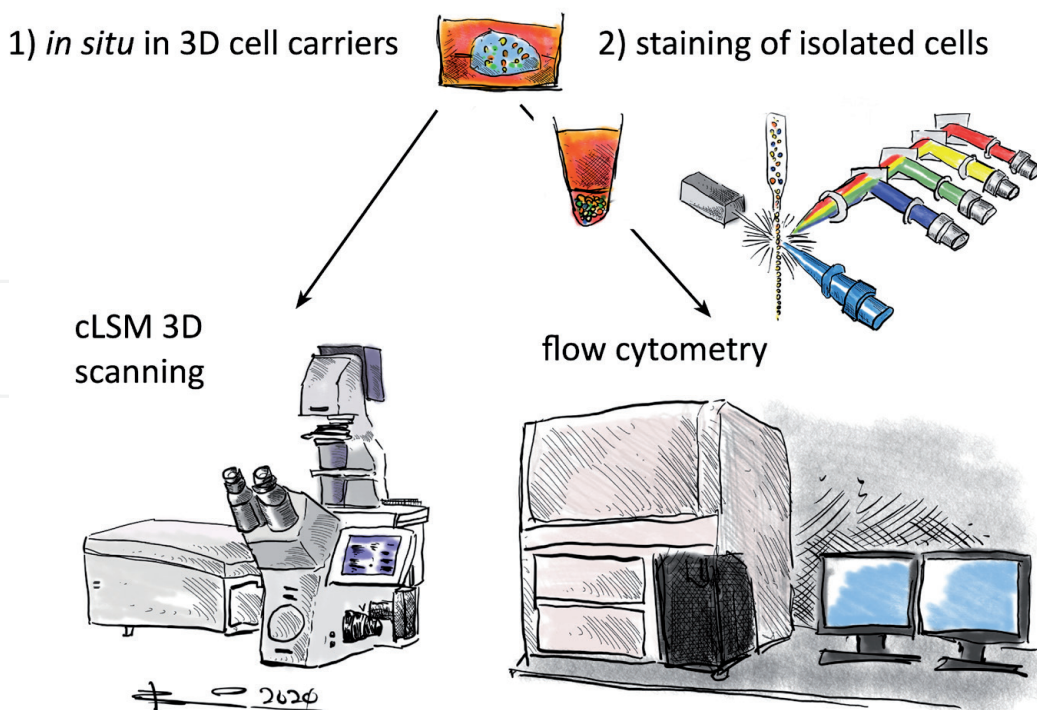


Figure 1. Overview of tissue engineering principles and judgement for cell viability (point out microscopy or FACS methods). The main decision is whether information on the cell morphology and spatial distribution is essential or whether quantitative numbers of CV are enough. In the latter case, determination of CV by flow cytometry using either fixed or live cells is the choice. However, in these cases the cells need to be isolated from the ECM firstly and then the 3D information and original cell morphology are lost. For certain applications in TE, it is crucial to see into the 3D distribution of living cells in the tissue/scaffold.

Staining	Name	λ_{Ex} [nm]	λ_{Em} [nm]	Providers	Applications and references
Calcein AM	Calcein acetoxyethyl ester (green)	496	516	Sigma-Aldrich, Thermo Fisher Scientific	Live cell staining, cell tracking [4, 16, 28–31, 43]
CellVue™	Claret far red linker kits	655*	675*	Sigma-Aldrich	Live staining [51]
DAPI	4',6-diamidino-2-phenylindole	340	488	Sigma-Aldrich, molecular probes, Thermo Fisher Scientific	Dead nuclei staining for fixed cells, does not stain live cells
DID	Vybrant™ Cell- Labelling Solutions (far red)	644	665	Thermo Fisher Scientific	Live/dead membrane staining [59]
DIL	Vybrant™ Cell- Labelling Solutions (orange)	549	565	Thermo Fisher Scientific	Live/dead membrane staining [59, 60]
DIO	Vybrant™ Cell- Labelling Solutions (green)	484	501	Thermo Fisher Scientific	Live/dead membrane staining [59]
EthD-1, EtDi	Ethidium homodimer-1	528	617	Sigma-Aldrich	Dead nuclei staining
LuminiCell Tracker™	Nanoparticles	422*	540*	Sigma-Aldrich	In vivo cell tracking
PKH26	Red fluorescent cell linker kits for general cell membrane labelling	551	567	Sigma-Aldrich	Live membrane staining, transplantation studies [53–56]
PKH67	Green fluorescent cell linker kits	490	502	Sigma-Aldrich	Live membrane staining [52, 60]

*Kits are available in multiple colours.

Table 1.

An overview of the most commonly applied fluorescent dyes to either determine cell viability (CV) or to track cells in scaffolds or tissues. Also given are whether they are more suitable for live cell imaging or to work with fixed cells.

fluorescent dyes are now also available from a wider range of distributors even as concentrated powders and can be bought for affordable prices. We would like to provide a series of more or less straightforward protocols to trace living cells in tissues, of which, we can provide our own experiences. Finally, we would like to conclude with some, in our view, hard-to-trace examples using biomaterials with strong autofluorescence or difficult optical characteristics. For these biomaterials, scanning may not be easy and no good workarounds exist yet.

1.2 Evaluation of the cell viability in hydrogels, living tissues and organs

In TE and for orthopaedics and other fields involving organ and tissue-oriented research, it is crucial to understand whether cells are alive if seeded into a scaffold and after a specific time of culture. For a cross-disciplinary field in regenerative medicine, it is essential to understand the viability of tissues and cells over time, especially in 3D scaffolds, where diffusion gradients arise through unequal distribution of nutrients, oxygen concentration and pH gradients caused by cellular

activity. TE frequently involves scaffold designing that then often needs to be assessed for cytocompatibility and cell viability. Thus, a central question is whether the spatial distribution of cells is essential or whether solely quantitative numbers are sufficient.

Currently, there are a number of assays available to determine CV in tissue or three-dimensional (3D) scaffolds, including lactate dehydrogenase staining (LDH) [32–34], calcein-AM with ethidium homodimer-1 staining, for example Live/Dead®, Ca-AM/EthD-1 and cell counting after scaffold/tissue digestion [35, 36] (**Table 1**). The easy and straightforward combination of Ca-AM/EthD-1 dyes can be used to stain living and dead cells directly in the scaffold or tissue. The Ca-AM is enzymatically hydrolysed into calcein in living cells, turning those into a bright fluorescent green. The EthD-1, on the other hand, is only able to enter cells with a compromised membrane and stains nucleic acid fluorescent red. It should be noted that it is also possible to count cells after scaffold digestion using different dyes or stains, which differentiate living from dead cells, such as Ca-AM or Trypan Blue (TB) [37].

There are many advantages of the LIVE/DEAD viability/cytotoxicity tests: One advantage is that the live cell staining is not dependent on cell proliferation and is a nonradioactive assay unlike thymidine uptake and ⁵¹Cr release assays [38–40]. Furthermore, stained cells can be observed using fluorescence illumination and can be counted to determine the percentage of viable (or non-viable) cells. For cells grown in multi-well plates, the overall fluorescence per well can be determined using a fluorescence plate reader. For 3D specimens, confocal laser scanning microscopy (cLSM) has widely been applied. The main advantage of the cLSM is its ability to record the precisely defined optical sections from a 3D sample. This can be achieved by moving the focal plane of the instrument stepwise through the depth of the specimen, whereby a series of optical sections (stacks) can be collected. This provides, of course, more detailed information than from a piece of tissue that contains data from only one focal plane [41, 42]. Because optical sectioning is relatively non-invasive, the 3D distribution and relative spatial relationship of stained living, as well as fixed, cells can be observed with reasonable clarity. Another essential feature is that the slices obtained by the cLSM can be forwarded to automated image analysis and can also be rendered as 3D stacks if the optical plains are sufficiently overlaid (about 20–30% is recommended). These stacks can then also be used to compute surface- or volume-rendered 3D reconstructions of the specimen. Accordingly, data from images can be processed and converted into cell counts and live/dead cell ratios, respectively.

Recently, the question was asked whether there are differences in outcomes among widespread cell viability techniques used in TE. To answer this question, three commonly used methods were recently systematically investigated: (i) classical hand counting by Trypan Blue and hemocytometer (ii) Live/Dead® staining in combination to confocal laser microscopy and (iii) lactate dehydrogenase (LDH) activity staining on histological slices (**Figure 2**) [16].

Generally, CV is defined as

$$CV = \frac{\text{number of living cells}}{\text{total number of cells}} \quad (1)$$

This formula is the basis to judge CV (Eq. (1)). The following paragraph will introduce the principles of live/dead staining and 3D scanning using cLSM technology, and provide hands-on protocols for staining connective tissues such as joints.

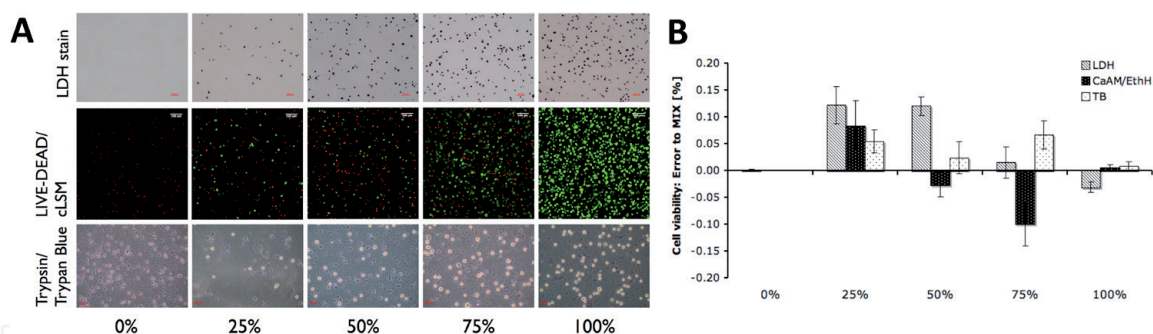


Figure 2. Representative images from the three different techniques used to estimate cell viability (i.e. LDH, Calcein AM/Ethidium homodimer (CaAM/EthD-1), and Trypan Blue staining after trypsin digestion) for five different cell viability mixtures, called MIX. (A) Exemplary images of cell viability stainings in fibrin 3D carriers using bovine chondrocytes. The pictures represent the outcome of an evaluation staining to control for cell viability (CV) and to investigate into the accuracy of these three prominent techniques to evaluate CV. (B) Error to MIX of the estimated CV in the MIX. It was evident that hand counting and Trypan Blue with hemocytometer is the most accurate method. CV was mostly overestimated with increasing number of living cells, especially with LDH assay. The figure was modified from [16] and reprinted with permission from the publishers. Values are means \pm SD, $n = 5$.

2. Applied protocols for live/dead staining of cells in tissues or scaffolds using cLSM

The following staining protocols using Ca-AM/EthD-1 in 3D carriers and tissues were partially reprinted with permission from the publishers. The protocols were modified and are based on the book chapter by [43].

2.1 Stage for 3D scanning

To ensure optimal optics, it is recommended not to use plastic well-plates from commercial manufacturers for scanning. Instead, a simple stage for 3D scanning with excellent optical characteristics for inverted microscopy can be produced with the following materials. The following protocol has been tested for intervertebral disc tissue of bovine and human origin but has also been successfully used for ligament tissue of human joints and cartilage biopsies.

1. Aluminium plate (dimensions 50 \times 80 \times 6 mm) (**Figure 3A and B**)
2. Metal drill to cut out a circular hole (\varnothing 22 mm)
3. Coverslip 30 \times 50 mm No.1 (e.g. Gerhard Menzel Glasbearbeitungswerk GmbH & Co. KG, Braunschweig, Germany)
4. Nusil[®] Medical Grade Silicon (MED-1137, Adhesive Silicone Type A, Silicone Technology, Carpinteria, CA, USA)

The Nusil[®] Medical Grade Silicon is dried for at least 72 hours.

The complete sample holder is washed twice with methanol and dried for 15 minutes before use (**Figure 3**).

2.2 Preparation of staining solutions

Prepare 1 mL of staining solution using serum-free Dulbecco's Modified Eagle Medium (DMEM) or phosphate-buffered saline (PBS) per tissue ($\sim 3 \times 3 \times 3$ mm³).

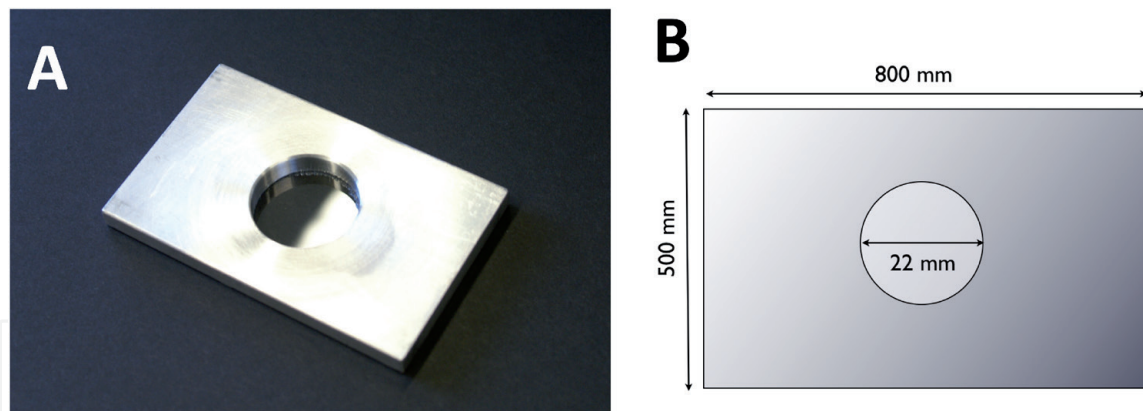


Figure 3. Customised sample holder for scanning tissues and scaffolds. Dimensions of simple custom-made sample holder (aluminium plate with 22 mm \varnothing drilled hole) used for improved 3D scanning. (A) Side view. (B) Schematic top view. The picture is modified but based on [43] and reprinted with permission from the publishers.

For the staining of tissue, we used a 10 \times higher concentration of Ca-AM (10 μ M) than usually indicated on live/dead kits. The reason for this increased concentration is the fact that the fluorescent molecule needs a longer time to penetrate into the tissue or carrier, and a higher concentration is needed. However, for the EthD-1, we kept a 1 μ M concentration as recommended by several manufacturers. Prepare the dye ‘cocktail’ directly before staining since fluorescent dyes are unstable in contact with water. Also, keep these freshly prepared dye solutions in the dark if possible.

2.3 Preparation of the tissue samples

IVD tissue from bovine or human origin or tissue of human ACL (in the latter case, both with ethical written consent) can be stained with this protocol, which we provide below. It is likely that incubation times and concentrations need to be adjusted for other tissue types.

1. Discs are then separated into nucleus pulposus and annulus fibrosus tissue by a 6-mm \varnothing biopsy puncher (Polymed, Glattbrugg, Switzerland).
2. Circular tissues are then further cut into half by a scalpel blade and annulus fibrosus is further dissected into inner and outer annulus fibrosus by eye.
3. Tissues pieces are emerged in 1 mL of a freshly prepared staining solution in a 12-well plate and incubated for 1 h at 37°C in 100% humidity and 5% CO₂.
4. After incubation, tissue bits are transferred into a fresh well-plate and washed with 1 mL of TBSS and checked immediately with the laser scanning microscope. For the imaging, a customised sample holder was used. The preparation of this customised sample holder is shown in **Figure 3**. For all of our live cell imaging, it was recommended to use a custom-made holder, which enables significantly improved optics than culture well-plates plastics on their own.

3. Staining and counting of pre-isolated fixed cells

In the following sections of this chapter, we present novel, unpublished data, and thoughts on the staining of fixed cells and how accurate these kits are to evaluate the CV in scaffolds and tissues. We used the new class of fixable dead stains with

the aim that CV could be determined in fixed tissues as an alternative to live/dead cell staining as outlined in the previous section. Fixable dead cell stains referred to as amine-reactive dyes (ARDs) are a class of viability dyes designed for the discrimination between living and dead cells in samples that will be fixed. It is a new class of viability assays using the principle of dead cell exclusion markers. The method is based on the reaction of a fluorescent reactive dye with cellular amines [44, 45]. The reactive dye crosses the compromised membrane of dead cells, thus reacting with free amines present in both the cytoplasm and the cell surface. This reaction leads to an intense fluorescent staining of the dead cells. On the opposite, living cells exclude this dye as their membranes are intact and only the cell-surface amines are available to react with the dye. This results in a significantly lower fluorescence signal, which is due to a fewer amount of amines reacting with the dye, as shown in **Figure 4**. The main advantage of fixable methods lies in the fact that the reaction is irreversible. Therefore, after cell fixation and permeabilisation, the bound dye remains linked with the dead cells and the staining is stable with no loss of fluorescence signal over a certain period of time [44, 45]. Moreover, ARDs are available in a variety of excitation and emission wavelengths, which gives a great advantage in terms of diversity, thus allowing a considerable flexibility when establishing staining protocols [44]. These cells will then be counted most efficiently using flow cytometry.

3.1 Cell viability mixtures

To evaluate different methods to estimate CV in terms of accuracy and precision, the approach is to generate, both, living and dead cell solutions that were then combined with pre-known CV ratios (PREMIX) 100%/0%, 75%/25%, 50%/50%, 25%/75% and 0%/100%. The preparation of the dead cells for the mixtures was performed based on the method by Gantenbein-Ritter et al. [16], where the non-viable cells were obtained by 1 N HCl treatment. It has been shown that cell nuclei stay intact with this method and, thus, can be detected with all methods under investigation. The cells were detached with 1% trypsin, centrifuged (500 g, 5 min) and then

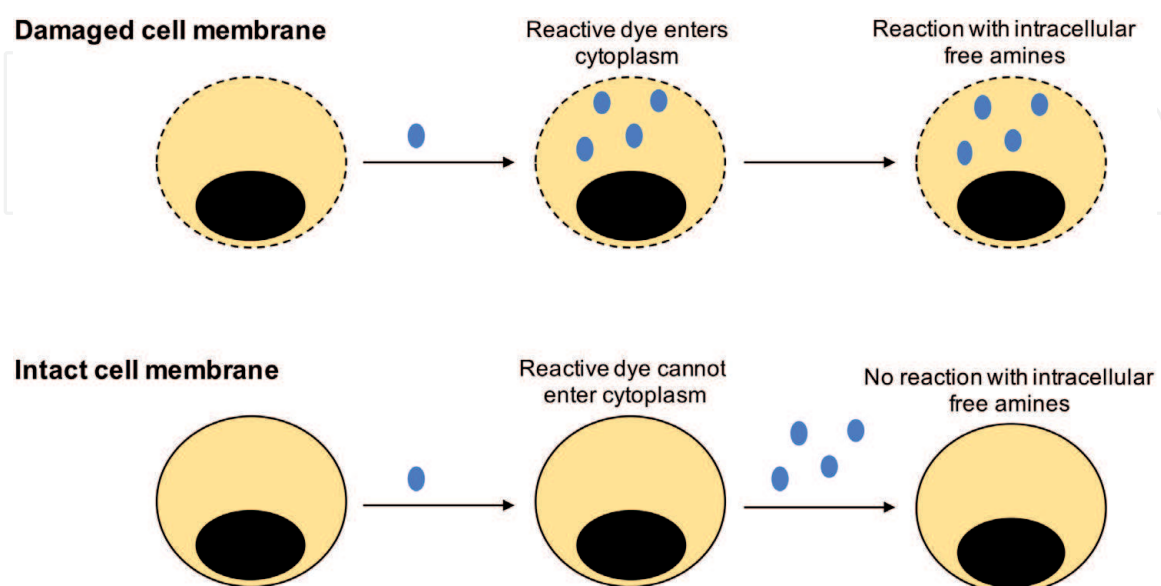


Figure 4. Principle of action of a fixable cell viability assay using amine-reactive dyes (ARDs). The top path represents cells with damaged membrane where the ARD (in blue) can enter into the cytoplasm. The bottom path shows living cells with intact cell membrane in which case the dye cannot pass. The principle is described in Perpetto et al. [45].

resuspended in PBS. The dying process was achieved by the addition of 1% of 1 N HCl in a PBS solution to the cell suspension followed by 10 min of incubation at room temperature (RT). The cells were then washed and resuspended in PBS. In parallel, living cells were detached, centrifuged (500 g, 5 min) and resuspended in PBS.

3.1.1 Amine-reactive dye (ARD) staining

In the following section, we describe how the ARD staining was evaluated for accuracy, and how it was compared to hand counting using TB and cLSM imaging.

3.1.2 Cell staining with ARD

For the comparison of the fixable versus the live cell imaging, the different cell mixtures were stained using the ViaQuant™ blue fixable dead cell stain kit from GeneCopeia (GeneCopeia, inc., Rockville, MD, USA). A cell density of 2×10^6 cells/mL for each mixture was used using ACL-derived ligamentocytes (LCs) and the staining protocol of the manufacturer's instructions was followed. In short, the cell suspension was incubated on ice and protected from light during 30 min in a 1-mL PBS volume where 1 μ L of dye was added. The cells were then washed with PBS prior to fixation with 3.7% formaldehyde during 15 min. Finally, the cells were used to prepare the CV ratios as described above for PREMIXes.

3.1.3 Cell labelling and gel casting to evaluate the ARD staining

Each cell suspension was added to 2% agarose (Lonza, Rockland, ME, USA) in a 1:1 ratio of 250 μ L volume to obtain a 1% agarose gel. The final cell density was approximately 2×10^6 cells/mL. Subsequently, 27 μ L of the agarose-cell mixture was then casted into a custom-made silicone mould (cylinder dimensions \varnothing 4 mm \times 2 mm height). After embedding into the gel, the cells were stained with the ViaQuant™ blue fixable dead cell stain kit and the pellets were incubated for 60 min in 1 mL of PBS containing 1 μ L of dye. In order to localise the cells in the 3D carriers, they were counterstained with EthD-1, which labelled all nuclei in red fluorescence. The cells were incubated for 5 min at RT in a 1-mL PBS solution containing 0.5 μ M EthD-1.

3.1.4 Hand counting method

With the TB method, the number of living and dead cells were manually counted with a Neubauer improved cell counting chamber by taking four repeated measurements of each cell suspension ($n = 4$ /suspension). The CV was computed for each count and then averaged. The hand counting procedure was then repeated after staining with ARD ($n = 8$ /cell mixture). In this case, cells were counted manually using a hemocytometer under a Leica DM IL microscope (Leipzig, Germany) using a blue fluorescence filter to determine the proportion of the two cell populations. Blue fluorescent cells corresponded to dead cells and the nonfluorescent ones to living cells.

3.1.5 cLSM imaging

The quantification of CV after ARD and EthD-1 staining of the 3D agarose carriers was performed using the ImageJ software (v1.51k, NIH) [27] by first obtaining the colocalised cells between the red and blue channels with the plug-in 'colocalisation highlighter'. Colocalised cells between EthD-1 and ARD staining corresponded

to the dead cells. For this purpose, the settings had to be adjusted in order to take into account only the bright blue fluorescent cells. The threshold values for both channels were set at 50% and two points were considered as colocalised if their respective intensities were strictly higher than the threshold of their channels. Dead cells were then counted using the plug-in 'nucleus counter'. The number of red cells corresponding to the total number of cells (living and dead) was also computed with the plug-in 'nucleus counter'. Thus, the number of living cells was obtained by subtracting the number of dead cells from the total number of cells.

4. Validation of cell viability methods

It is important to know the accuracy and precision of the most commonly applied cell viability methods in the laboratories. Here, we summarise the results of two studies, one involving the comparison of several live methods, that is, Trypan Blue staining and manual cell counting using hemocytometer (TB), live/dead staining, and cLSM imaging (CA-AM/EthD-1). The second study, we present here, is on the usage of ARD stains and its accuracy for CV in comparison to live/dead staining followed by cLSM and was not published previously.

In the case, where CV is then quantified in 3D using a cLSM microscope, the following procedure was applied: Firstly, the stacks were separated into separated channel images and the CV was determined on each of the images (Figure 5). This step was done using the open source macro of ImageJ. In this routine, the red and green cells were quantified separately per single image using a custom-made macro in ImageJ software named 'Cellcounter3D' (deposited at <http://imagej.nih.gov/ij/macros/Cellcounter3D.txt>) and available free of charge under the GNU licence [16]. The macro consists of a converting step to 8-bit mode and a threshold step that passes a binary image with pixels in the range of 100–255 to the plug-in 'nucleus

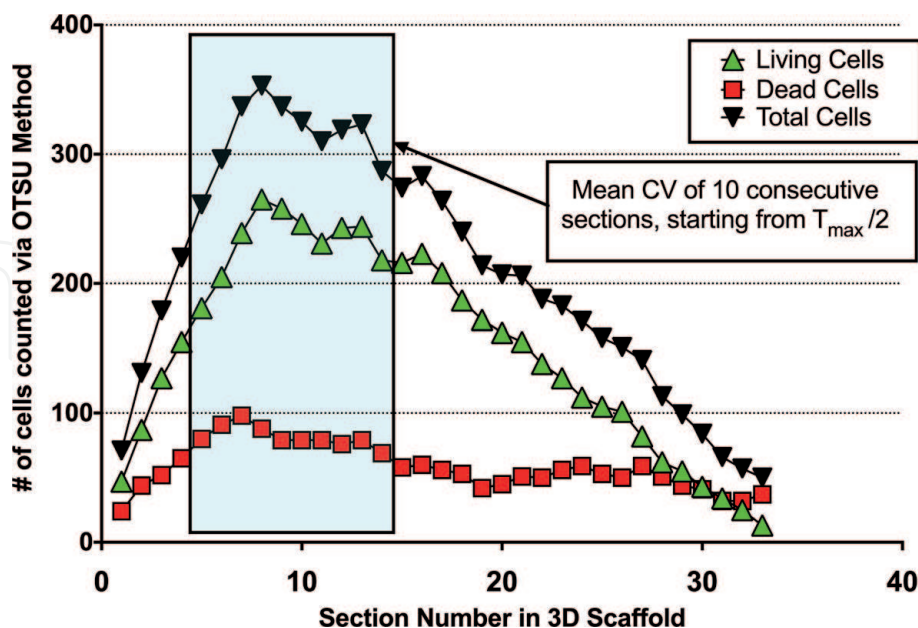


Figure 5. Progress of cell viability (CV) estimates through a 3D stack using the custom-written 'Cellcounter3D' routine of imageJ and the OTSU method to count the number of green (live cells), red (= dead cells) and the total number of cells in z-stacks of cLSM images. As can be seen, the total number of cells increases after about 5–10 sections inside the scaffold and then reaches a plateau of about 10–15 consecutive optical sections. The first five images from the tissue surface are rejected as these are prone to error due to cell death by tissue/carrier manipulation. In light blue is the window indicated that is then used to estimate the CV of 10 consecutive pictures after the maximum of the total cell number reached $T_{max}/2$. The picture is based on [43] and has been reproduced with permission from the publishers.

counter' (available at <https://imagej.nih.gov/ij/plugins/mbf/index.html>). This step then uses the 'Otsu' method for particle counting [46]. The minimum and maximum island sizes were set to 7–50 and 15–100 pixels for the red and green channel, respectively. Please, note that these parameters can be modified dependent on the quality of a specific hydrogel/biomaterial and dependent on the cell density and the type of cells seeded. It is important to inspect the segmentation and cell counting progress by eye to judge whether the numbers are meaningful. The intermediate steps like the results of the segmentation progress can be also stored as .tiff or .jpg files for further documentation.

In the following steps, we describe the settings to determine CV using live/dead staining and cLSM technology. The 3D carriers were produced using a mould, made of easy-sterilisable materials, such as silicon membranes or stainless steel. The dimensions of these moulds were in this case of a cylindrical shape of 4 mm in $\varnothing \times 2$ mm in height, corresponding to a volume of 27 μL of carrier. The final chosen cell density was 2×10^6 cells/mL. The 3D carriers, that is fibrin, PEG or 1% agarose, respectively were cut sagittally into halves and incubated in 1-mL high glucose Dulbecco's Modified Eagle Medium (DMEM) without fetal calf serum (FCS) containing 10 μM CaAM and 1 μM EthD-1 (both Fluka, Sigma-Aldrich, Buchs, Switzerland) for 3 h at 4°C followed by 1 h of incubation at 37° C, 5% CO₂ and 100% humidity. The carriers were then scanned from top and bottom surfaces to ~200 μm depth at two random locations per side with a confocal laser scanning microscope (cLSM510, Carl Zeiss). Stacks were taken at 10 \times magnification at a 512 \times 512 pixels resolution (field size of 921.4 \times 921.4 μm) with the pinhole at 1 Airy unit and 50% image overlap and 5.8- μm intervals. The proposition was then to quantify CV on a subset of 10 consecutive images, starting at the image with 50% or more of the maximum amount of the total cells per image in a single stack (**Figure 5**). Additionally, the first five sections starting from the surface into the scaffold were also rejected as there cell death occurred through tissue manipulation, which causes a strong bias. To determine this frame, a MatLab routine has been written (MatLab R2020a, MathWorks inc., Natick, MA, US), which picks the analysis-window automatically and summarises the CV results in a compact table. The code is available free of charge at the Mathworks repository under the keyword 'Cell Viability Estimator for 3D Scaffolds' [47]. **Figure 5** illustrates a typical profile through a stack of images for the living, dead and total cells. The cells in this case were bovine chondrocytes from articular cartilage seeded at a cell density of 4 M cells/mL in fibrin hydrogel (Tisseel™, Baxter, Vienna, Austria) according to a customised recipe as described in [16]. These cells were counted then using three different methods on day one of culture under standard conditions. It is important to note that CV can be determined also on z-compressed images, which represent a cumulative summary of the entire stack or on individual scans through the stack as introduced here.

The accuracy of the dead cell fixable viability assay was then determined by computing the relative error between the theoretical cell viability and the hand counting, flow cytometry and cLSM results obtained after the ARD staining. The theoretical viability was based on the hand counting of living and dead cells of the different cell mixtures with the TB method. Then, the relative error (Δx) was computed as followed in Eq. (2):

$$\Delta x = \left| \frac{x_0 - x}{x} \right| \quad (2)$$

where, x_0 corresponds to the CV measured with any of the to be compared methods, that is, LDH, ARD+FACS, cLSM live/dead and compared to x , the one from the TB assay known as the reference method (=PREMIX).

The accuracy of all the methods was quantified in regards to the cell mixtures by calculating the absolute error (δx) as followed in Eq. (3):

$$\delta x_{i,j} = \bar{x}_{i,j} - p_i \quad (3)$$

where $x_{i,j}$ is the mean CV of each method, j , and p_i are the estimated CV of the prepared cell mixtures, i .

5. Comparisons of CV estimation methods

It was recently found in an earlier study that in a systematic comparison of Trypan Blue, CA-AM/EthD-1 by 3D stack scanning with lactate dehydrogenase activity on cryosections and lastly vs. and averaging [16] and thirdly by comparing lactate dehydrogenase (LDH) activity and ethidium homodimer-1 co-staining and using histological sectioning. What is needed in such studies are known cell premixes (in short MIX) to determine the error. In this study, it became evident that LDH and Ca-AM/EthD-1 methods overestimated the number of living cells with respect to MIX in all cell viability mixtures (except for 0%), whereas TB method always slightly underestimated this number; however, it was clearly the one closest to the MIX values. **Figure 5** illustrates how premixes of known living and dead cells can be produced and then how three particular different live/dead staining (methodologies) were compared. In this comparison, it became evident that optical methods such as cLSM have a relatively high deviation from the MIX as it was overestimating the total number of cells per volume by a factor of about four. The reason for this was attributed to the refraction index of the IVD tissue and/or the hydrogels that might cause an experimental bias.

5.1 Flow cytometry

Flow cytometry analysis of the different CV mixtures was correlated with certain variations of the aimed living/dead cell ratio. The results were different

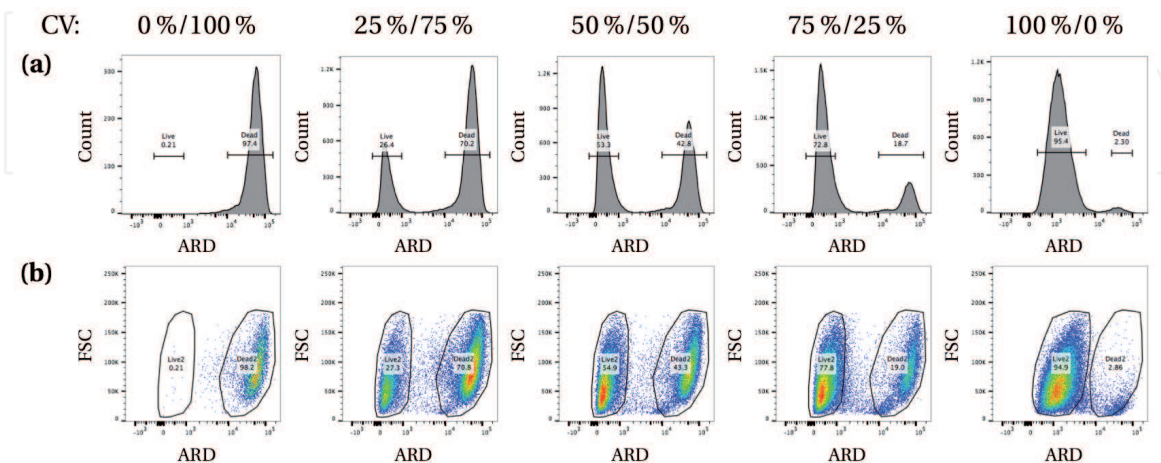


Figure 6.

Flow cytometry results for isolated primary human cells from the anterior cruciate ligament (ACL) cells, which were stained at different PREMIXes of living and dead cells, that is, 100%/0%, 75%/25%, 50%/50%, 25%/75% and 0%/100% and then stained with the ARD. CV can then be inferred from either (a) histogram of the ARD and cell counts with the different peaks depending on the cell populations (FACS-2D plot) or from (b) 2D (with the dimensions plots of the ARD and forward scatter (FSC) with the two distinct populations according to the CV mixture (FACS – histogram plot)). However, these are only minor deviations between the two methods, which arose from the variation in the gating.

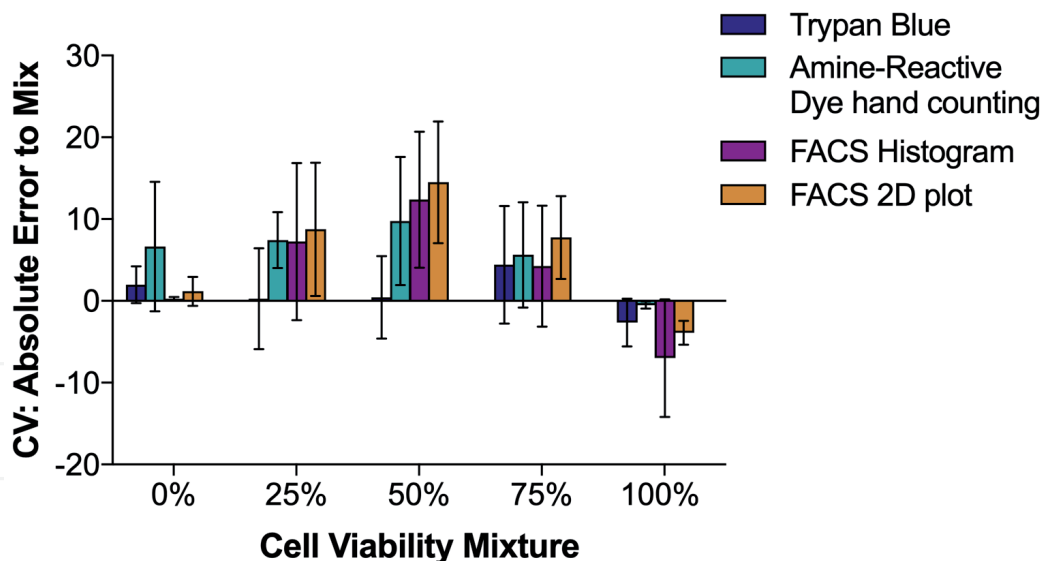


Figure 7. Results of absolute error relative to the prepared mixtures for CV measurement determined with the four different methods: TB assay, hand counting with ViaQuant™ staining, FACS-histogram and FACS-2D plot illustrating the determination of the gates for live and dead cells. Values are presented as mean \pm SD, $N = 4$.

depending on the representation of the data with either the histogram (**Figure 6a**) or 2D plot (**Figure 6b**), but they stayed in a close range. Both representations revealed an overestimation for the 0%, 25%, 50% and 75% targeted CV, but for 100% CV mixture, the result was underestimated.

5.2 Accuracy of fixable viability assay

The accuracy of the fixable viability methods was tested by comparing the computed viability of the different methods to the theoretical viability, based on the TB assay. All CV mixtures matched the targeted CV with variations among some ratios and methods, as depicted in **Figure 7**.

6. Cell tracking methods: colocalisation of fluorescence

There are study designs that require cell tracing methods. For instance, isolated cells from species in which they are labelled with non-specific membrane dyes or organelle dyes. In this case, cells from species (or an individual) A are transplanted into species (or an individual) B and are then monitored over time with respect to cell viability [48, 49]. This could be of particular importance in the case of autologous or allogeneic stem cell research, where for instance, mesenchymal stromal cells (MSCs) are transplanted into live organisms or in vitro using organ culture systems. Here, long-lasting fluorescent dyes are the method of choice. It has been characterised in a number of model systems and has been found to be useful for in vitro cell labelling, in vitro proliferation studies and long-term, in vivo cell tracking [50]. Here, dyes such as PKH26 or PKH67 (PKH26GL, Sigma-Aldrich, Buchs, Switzerland), and CellVue® Claret are commonly used [51–55] (**Table 1**). The half-life for the elution of red-fluorescent lipophilic membrane dye PKH26 from labelled rabbit red blood cells is greater than 100 days. PKH26 was used also to stain extracellular vesicles of mammalian cells [56]. It has been recently found that this particular dye seems to leak into non-stained cells in vitro and in vivo [54]. Furthermore, the staining involves a step, where cells are exposed for about 5 min in a diluent, which is

highly hydrophobic and is known to cause cell stress and therefore potentially influences the outcome. Thus, exposure in this staining process needs to be optimised for each cell type (User bulletin of Sigma-Aldrich [57]). Less cytotoxic seems to be, at least from our experience, the carbocyanine dyes like the product from Vybrant™ Cell-Labeling Solutions (Molecular Probes, Thermo Fisher Scientific, inc., a multicolor kit available under cat#V-22889) [58]. There is a notable selection of these dyes, including DiI ($\lambda_{Ex} = 549$ nm; $\lambda_{Em} = 565$ nm; in blue range emission), CM-DiI, DiO ($\lambda_{Ex} = 481$ nm; $\lambda_{Em} = 501$ nm; orange-red emission) and DiD ($\lambda_{Ex} = 644$ nm; $\lambda_{Em} = 655$ nm; dark red range emission). In the case of CM-DiI ($\lambda_{Ex} = 553$ nm; $\lambda_{Em} = 570$ nm; red range emission), the cells can be traced even after fixing and paraffin embedding [59, 60] (Table 1). These dyes do not need to go through a rather stressful staining step in a strong solvent, a feature that is welcome for many cell tracing experiments, where the transplanted tissue cannot be scanned immediately after the experiment on a certain time point. Our previously presented imageJ macro 'Cellcounter3D' (available from: <http://imagej.nih.gov/ij/macros/Cellcounter3D.txt>) also allows to count multiple single channels. We recommend to use the plug-in 'LSM_Batch_with_colors.txt', which can be also obtained from the ImageJ repository, to split the channels firstly. If multiple dyes and channels are being used, it is recommended to split the channels into single .tiff or .jpg images with increasing indices of the z-stack images. Then, there are also plug-ins for colocalisation, such as the 'colocalisation finder', which was found to be highly useful, as these allow to define the pixels with colocalised stainings. In the case of PKH26 or DID stained cells, thus cells in the red wavelength range for instance in combination of Ca-AM staining, the number of 'yellow' stained cells should be counted. With this open source solution it is possible to distinguish for instance injected viable cells that show Ca-AM staining and cell tracer labelling (green + red stained = yellow), live native cells (green only) and dead injected cells (red only cells), and 4',6-diamidino-2-phenylindole (DAPI) was used to counterstain for dead cells, thus, blue only cells are to be considered 'native' or autochthonous dead cells. These concepts were applied in studies where stem cells needed to be traced after injection into an IVD organ culture model [48, 61]. Here, it was possible to trace cells inside an organ culture system of an IVD, labelled with the proposed dyes and colours.

7. Real-time microscopy using cell fluorescent dyes

Lately, it has become fashionable to monitor cell proliferation using a selected number of time points but using real-time imaging and using cell tracing/tracking experiments. Several microscopes offer now high-throughput approaches to monitor cell proliferation and cell death over time. Here, two devices are of interest to be mentioned: one is the Nikon Biostation CT (Nikon, Tokyo, Jp) and the Incucyte S3 (Essen BioScience, Ltd., Newark Close, UK) with three fluorescent channels (note: the latest release S5 comes even with five channels). There are also several more affordable devices on the market, which, however, do not allow to track multiple culture vessels and cell conditions at the same time but rather single vessel monitoring over time. Real-time monitoring of cell shapes turned out to be very useful to monitor for instance MSCs undergoing differentiation as it was possible to discriminate differentiating cells according to certain 'features' using segmentation methods and statistical shape modelling [62]. MSCs could also be traced in dependency of their passaging number, that is, in dependence of their senescence [63]. These cell motility pathways were tracked for instance

using ImageJ [27] and the open source plugin ‘MTrackJ’, which allows manual tracking of individual cell trails. More recently, fast microscopes were designed that can handle high-throughput monitoring of multiple wells, and even multiple spots of interest in the well. Here, we can report on the experience with the use of the Incucyte S3 (Essen Bioscience), which in our hands, produced highly satisfactory results for cell tracing in co-culture experiments with direct cell–cell contact. As an example, the cytoplasm green of bone marrow-derived MSCs was stained with IncuCyte® CytoLight Rapid Green Reagent, cat# (cat. No. 4705). Additionally, primary human nucleus pulposus cells (NPCs) of the IVD were stained with IncuCyte® CytoLight Rapid Red reagent (cat. No. 4706). These cells were then seeded in 96-well plates in a ‘race’ experiment seeding 50:50 with 4000 cells per cell type, and the interactions and the cell proliferation between the two cells was monitored (Video 1). Both cell types were cultured in an osteogenic medium, which was alpha-Modified Eagle Medium (α MEM, Gibco, Thermo Fisher Scientific) supplemented with β -glycerophosphate, dexamethasone and vitamin C to thrive MSCs towards osteogenic differentiation. The presence of red NPCs was added in this experiment to monitor the inhibitory effects of these onto the MSCs undergoing ossification. We have previously shown that IVD cells such as NPCs can inhibit MSCs undergoing ossification by expressing BMP antagonists [64, 65]. As for the fluorescent stainings in this case, it became evident in this experiment that both dyes are washed out in less than 12 h of culture. **Figure 8** illustrates the cytoplasmic stains on MSCs (in green) and NPCs (in red) and how the staining faints after only a few hours by cell divisions in the co-culture. Thus,

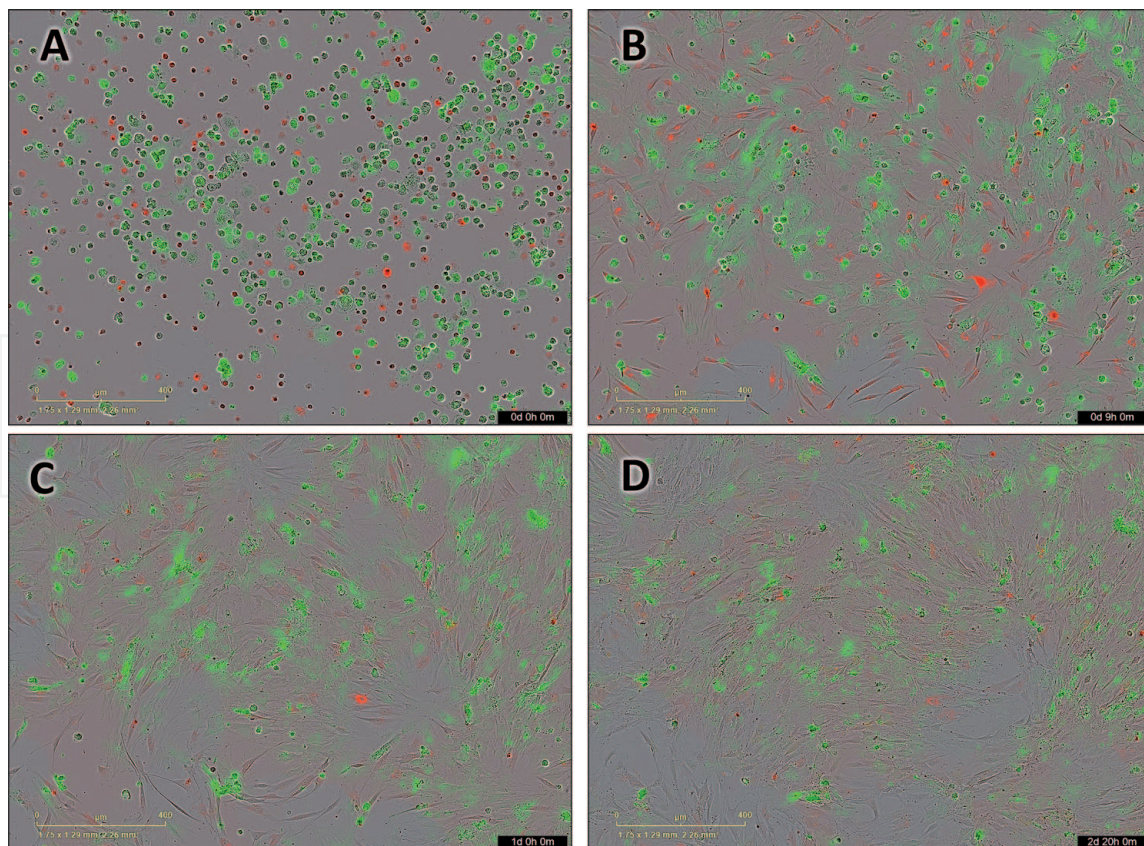


Figure 8. Phase-contrast microscopic images of time-lapse microscopy of a co-culture of human MSCs (stained in green) with NPCs (stained in red) seeded in a 1:1 ratio. (A) Status immediately when cells were seeded at time point 0; (B) cell populations after 9 hours; (C) Cell populations after 24 hours; and (D) cell populations after 2 days and 20 hours in culture. Please, note how the red cytoplasmic staining faints more rapidly over time than the green staining of the MSCs. Fluorescence staining must be optimised for each cell type separately.

these stainings from Essen Bioscience would need to be optimised for long-term experiments for several weeks.

8. Trouble shooting of difficult carriers with strong fluorescent interference

In some cases, unexpected problems were encountered with special biomaterials, which hindered any kind of CV designation as presented above using classical live/dead stain. For instance, staining for cyto-compatibility is often done on 3D hydrogels and other 3D biomaterials that do not allow a transparent view. In the case of *Bombyx mori* silk, for instance, it was found that staining with EthD-1 was not possible due to a very strong autofluorescence of the silk material (**Figure 9A and B**). Moreover, integration of genipin, which is a natural cross-linker to increase stiffness of hydrogels, has been proposed [66–69]. The increasing concentration of genipin leads to increasing autofluorescence, noticeable as ‘noisy background’ on the red fluorescent channel. This can be seen in **Figure 9C**, where MSCs were stained with Ca-AM life staining but the genipin-reinforced fibrin hydrogel was making it impossible to use EthD-1 as the second dye to visualise dead cells. Therefore, DAPI (blue)

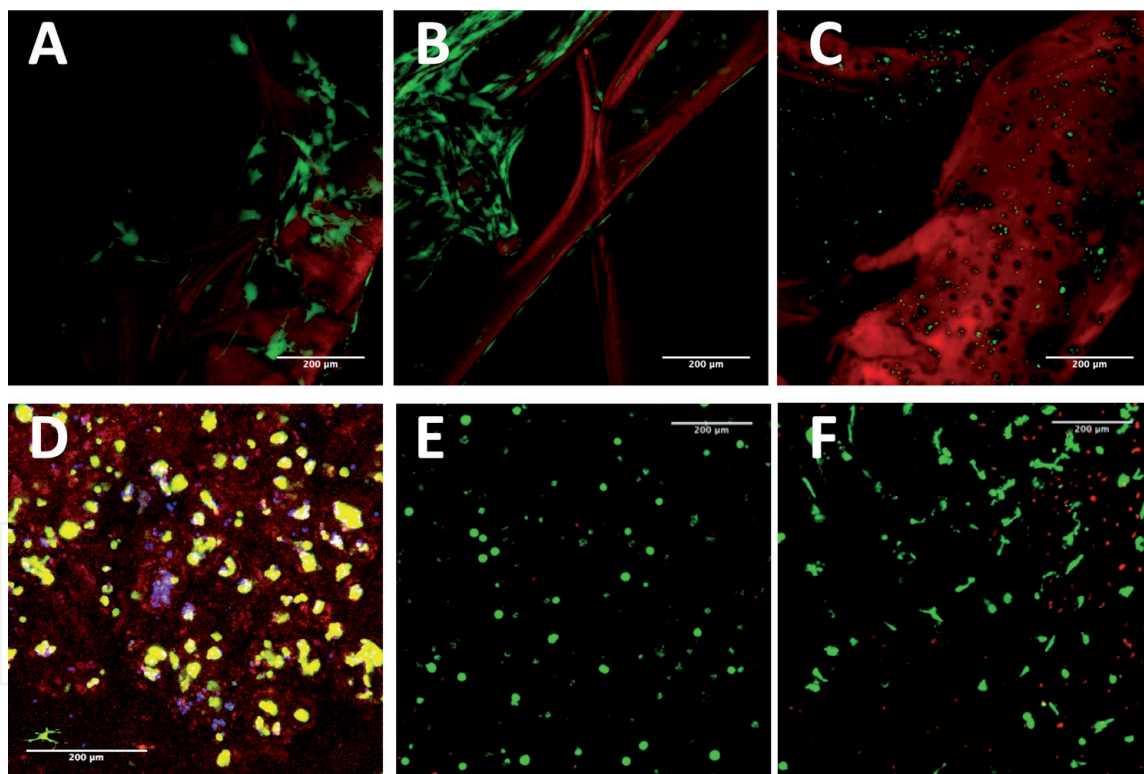


Figure 9.

*(A–C). Examples of difficulties to quantify cLSM 3D-scan projections on complex biomaterials. Pictures represent z-stacks of compressed images through a stack of ~200 μm through the respective biomaterials. Primary human-derived bone marrow mesenchymal stromal cells (MSCs) were seeded and cultured for 21 days on (A) silk-fleece from *Bombyx mori* (produced from Spintec engineering, GmbH, Aachen, Germany) (in red with strong autofluorescence from the silk material [18]); (B) human MSCs on *B. mori* silk after 21 days of culture containing growth factor GDF6 (naturally expressed by Baculo-virus transduced *B. mori* larvae that co-expressed the human growth factor during larval growth); (C) human MSCs cultured in fibrin hydrogel (45 mg fibrinogen/mL, Tisseel™, Baxter) containing 4.5 mg/genipin, a natural cross-linker to stiffen the hydrogel. Notice, the strong red staining resulting from the genipin cross-linker in the hydrogel [67]. (D) Example of an image with co-staining of injected cells into an organ, that is isolated progenitor cells stained with DID (Vybrant™, thermo Fisher scientific) and calcein AM into IVD; (E) human NPCs cultured for 21 days in polyethyleneglycol hydrogel (PEG) lacking RGD motive (Q-gel™); (F) human NPCs cultured for 21 days in PEG hydrogel with RGD motive, showing filopodia growth. Cells adhere with filopodia to the matrix and change to a very artificial cell phenotype [17].*

ore an alternate dead staining needs to be taken. The feature of intrinsic fluorescence of genipin was recently proposed as a wanted side effect for *in vivo* studies to track hydrogels [70]. **Figure 9D** is an example of an experiment, where a hydrogel, in this case a methacrylated gellan gum [71, 72], is used as a carrier material and mixed with bovine nucleus pulposus progenitor cells (NPPCs) [73]. This mix was then injected into a bovine IVD organ culture model. The aim was to determine the CV and to identify and distinguish transplanted and native cells. The cells were monitored for live/dead staining after 2 days of organ culture [61]. The cells were labelled with DID and CaAM prior injection and resulted in yellow co-labelled cells. **Figure 9E** and **9F** demonstrates the effects of integration of cell adhesion motives by lack (**Figure 9E**) or integration of RGD (**Figure 9F**) into a commercially available hydrogel made of high-molecular weight polyethylene glycol (PEG) (QGel™, QGel inc., Lausanne, Switzerland). Due to the addition of the RGD, NPCCs started to develop filopodia, which is a very unnatural cell shape and morphology for these cells. This feature, however, may be very useful if MSCs are cultured in 3D depending on the specific research question under mechanical loading [17].

9. Discussion

CV is a very central parameter in TE methods. However, this parameter is prone to multiple sources of errors. Errors come in not only from the methodology, the experimental design, the experimenter, but also from the technical limitations of the devices. Here, we presented our data for the systematic evaluation of some of the more commonly applied methods.

First of all, there are various methods, which allow inferring cell viability. Here, we discussed direct methods, which use fluorescent dyes such as Ca-AM or similar dyes or combined with membrane dyes. Depending on the research question, a major factor is whether the morphology and the spatial distribution matters (**Figure 1**). Then, fluorescent dyes combined with microscopic techniques are the methods of choice. To get dynamic CV quantification in 3D stacks, it is even recommended to use cLSM technology, which will give a very accurate visualisation of the CV in depth. The disadvantage of this methodology is clearly that the tissue needs to be stained right away after stopping the experiment, and the scanning should take place within 1–2 h after the staining procedure. Samples should be kept if possible at 37°C and the laser exposure inside the cLSM should be minimised.

Alternatively, tissue fixation and subsequent CV quantification has the advantage that any microscopic analyses can be postponed for a future time point.

Either tissue fixation or freezing in O.C.T. compound is an option (Tissue-Tek® O.C.T.™ Compound, AJ Alphen aan den Rijn, The Netherlands). These scaffolds then need to be cut using a cryotom. The samples can then be stained with other live stains using LDH assay (usually a brownish formazan staining) in combination with a dead cell staining, for instance DAPI (blue) or EthD-1 (red).

ARD stains that are applied onto cells did not seem to work for any kind of tissue staining (tested were IVD and ACL tissue). However, if cell morphology does not matter and cells can be successfully isolated by mild digestion (e.g. by pronase/collagenase digestions overnight) [74] without losing the dead cells in the digestion process, this could become a valid alternative to live/dead imaging. However, the protocol for ARD stain works perfectly for flow cytometric applications (see **Figure 6**). We have also evaluated the stability of the ARD for later FACS analysis. Fluorescent ratios and intensities remained unchanged if stored at 4°C after 7 days (our data not shown). Interestingly, CV is overestimated for most methods (**Figures 2** and **7**). As seen for all of

our comparisons in terms of accuracy, the TB method was performing best. If the ARD dye was used in hand counting methods, it also overestimated the true CV (**Figure 7**).

It can be complex to determine CV in cell suspensions and in tissue samples, as there are two modes of cell death: necrosis and apoptosis [75, 76]. Necrosis is an uncontrolled cellular death where cells lose their membrane integrity, whereas apoptotic cells die in a controlled manner involving cell shrinkage, nuclear fragmentation and the formation of apoptotic bodies [75]. Most of CV assays such as dye exclusion or intracellular enzyme release rely only upon necrotic loss of membrane integrity, thus omitting the detection of apoptotic cells. To detect apoptotic cells, other fluorescent-based kits are recommended such as the detection of caspase 3 activity [22].

Thus, future methods will consider fluorescent methods in the tissue and directly distinguish apoptosis and necrosis. It could involve the application of assays detecting only apoptotic cells such as it is the case in the TUNEL assay. In this case the detection of cell undergoing apoptosis is achieved through the use of modified nucleotides and enzymes to label DNA fragments. DNA fragmentation is detected by labelling the 3'-hydroxyl termini in the double-stranded DNA breaks that are generated during apoptosis. In the case of flow cytometry study, annexin V would also be a possibility as it is an early marker of apoptosis. It binds to phosphatidylserine, which is a marker of apoptosis when it is present on the outer part of the plasma membrane. It should be noticed that recently a third form of cell death has been defined, which differs from apoptosis and necrosis, which is called 'autophagy'. Autophagy differs from the previous forms in that cells can be killed by starvation from particular growth factors and cellular stresses [75].

Live/dead staining can only discriminate in a limited way between necrosis and apoptotic cell death. Autophagy cannot be distinguished with the fluorescent dyes described in this chapter. It could be feasible to address apoptotic cells using cLSM if certain cell nuclei demonstrate fragmentation of the nuclei. However, most dead cells by image segmentation methods that will be identified will have died through necrosis and show a clearly structured nucleus. As it was mentioned in the introductory chapter, an improvement of the reliability can be obtained by combining various CV methods [22, 77]. Thus, the use of the fixable dead cell stain would be best when used in combination with another CV assay or live and dead staining.

10. Conclusions

- CV can be determined with a wide range of methods allowing to stain mammalian cells. However, which techniques should be used is determined from the question at hand.
- TB method, a relatively cheap and affordable method, was the most accurate method to evaluate PREMIXes in all of the previous investigations.
- Live/dead imaging and cLSM imaging using 3D stacks is a very suitable method to quantify CV in 3D scaffolds. The samples with cells embedded in 3D hydrogel carriers or also native in the tissue can be scanned by cLSM about 300 μm deep into the tissue.
- cLSM scanning requires good optics. The total cell number per volume was overestimated by a factor of four for yet unconfirmed reasons, possibly deviations from the refraction indices of hydrogel-like materials.

- Cells can be traced using membrane dyes, such as PKH26, DID, DIO, DIL or similar dyes. Staining protocols for each specific mammalian cell type might have to be optimised.
- Fixable dead cell staining kit, as for instance the ViaQuant™, is optimised for flow cytometric analyses, and can only be partially used for TE applications. Its application for tissue samples is not possible as the dye cannot specifically stain dead cells.
- Rather, this fixable kit is more suitable for toxicology screening where cells are kept in suspension. It still has some advantages over other viability assays like flexibility of the experimental design in terms of excitation wavelength and stability of the dye after fixation, and also its simple handling.

Acknowledgements

This work was supported by the Swiss National Science Foundation grant number 310030E_192674/1 and by a start-up grant from the Center for Applied Biotechnology and Molecular Medicine (CABMM) to B.G.

The authors thank Daniela D. Frauchiger, Silvan Heeb, and Rahel D. May for the contribution of the images/movies involving silk or genipin-reinforced fibrin hydrogel. They are grateful to László Kupcsik and Marije de Jong (Van der Werf) for the assistance in the development of the ImageJ ‘Cellcounter’ macro and the MatLab routine ‘Cell Viability Estimator for 3D Scaffolds’ for CV determination for cLSM analysis. The cytometer equipment was from FACSlab core facility of University of Bern (www.facslab.unibe.ch). The microscopes were provided by the microscope core facility of the University of Bern (www.mic.unibe.ch).

Conflict of interest

The authors declare no conflict of interest.

Abbreviations

ACL	anterior cruciate ligament
α MEM	alpha-modified eagle medium
ARD	amine-reactive dye
Ca-AM	calcein acetoxymethyl ester
Ca-AM/EthD-1	calcein acetoxymethyl/ethidium homodimer-1 = LIVE/DEAD staining
cLSM	Confocal laser scanning microscopy
CV	cell viability
DAPI	4',6-diamidino-2-phenyl-indole
EthD-1	ethidium homodimer-1
FACS	fluorescence-activated cell sorting
FCS	fetal calf serum
IVD	intervertebral disc
LC	ligamentocyte
LDH	lactate dehydrogenase
LG-DMEM	low-glucose Dulbecco's modified eagle's medium

MSC	mesenchymal stromal cell
PREMIX	the pre-made mixtures of live and dead cells to determine the accuracy of methods
NP	nucleus pulposus
PBS	phosphate-buffered saline
RT	room temperature
SD	standard deviation
TB	Trypan Blue

IntechOpen

Author details


Benjamin Gantenbein^{1,2*}, Andreas S. Croft¹ and Marie Larraillet¹

1 Department for BioMedical Research (DBMR), University of Bern, Bern, Switzerland,

2 Department of Orthopaedic Surgery and Traumatology, Inselspital, University of Bern, Bern, Switzerland

*Address all correspondence to: benjamin.gantenbein@dbmr.unibe.ch

IntechOpen

© 2020 The Author(s). Licensee IntechOpen. Distributed under the terms of the Creative Commons Attribution - NonCommercial 4.0 License (<https://creativecommons.org/licenses/by-nc/4.0/>), which permits use, distribution and reproduction for non-commercial purposes, provided the original is properly cited. 

References

- [1] Hohlrieder M, Teuschl AH, Cicha K, van Griensven M, Redl H, Stampfl J. Bioreactor and scaffold design for the mechanical stimulation of anterior cruciate ligament grafts. *Bio-medical Materials and Engineering*. 2013;**23**(3):225-237. DOI: 10.3233/BME-130746
- [2] Nöth U, Schupp K, Heymer A, Kall S, Jakob F, Schütze N, et al. Anterior cruciate ligament constructs fabricated from human mesenchymal stem cells in a collagen type I hydrogel. *Cytherapy*. 2005;**7**(5):447-455. DOI: 10.1080/14653240500319093
- [3] Petrigliano FA, McAllister DR, Wu BM. Tissue engineering for anterior cruciate ligament reconstruction: A review of current strategies. *Arthroscopy*. 2006;**22**(4):441-451. DOI: 10.1016/j.arthro.2006.01.017
- [4] Lightfoot A, Martin J, Amendola A. Fluorescent viability stains overestimate chondrocyte viability in osteoarticular allografts. *The American Journal of Sports Medicine*. 2007;**35**(11):1817-1823. DOI: 10.1177/0363546507305010
- [5] Mohanraj B, Hou C, Meloni GR, Cosgrove BD, Dodge GR, Mauck RL. A high throughput mechanical screening device for cartilage tissue engineering. *Journal of Biomechanics*. 2014;**47**(9):2130-2136. DOI: 10.1016/j.jbiomech.2013.10.043
- [6] Stoddart MJ, Grad S, Eglin D, Alini M. Cells and biomaterials in cartilage tissue engineering. *Regenerative Medicine*. 2009;**4**(1):81-98. DOI: 10.2217/17460751.4.1.81
- [7] Behrendt P, Ladner Y, Stoddart MJ, Lippross S, Alini M, Eglin D, et al. Articular joint-simulating mechanical load activates endogenous TGF- β in a highly cellularized bioadhesive hydrogel for cartilage repair. *The American Journal of Sports Medicine*. 2020;**48**(1):210-221. DOI: 10.1177/0363546519887909
- [8] Haglund L, Moir J, Beckman L, Mulligan KR, Jim B, Ouellet JA, et al. Development of a bioreactor for axially loaded intervertebral disc organ culture. *Tissue Engineering. Part C, Methods*. 2011;**17**(10):1011-1019. DOI: 10.1089/ten.TEC.2011.0025
- [9] Rosenzweig DH, Gawri R, Moir J, Beckman L, Eglin D, Steffen T, et al. Dynamic loading, matrix maintenance and cell injection therapy of human intervertebral discs cultured in a bioreactor. *European Cells & Materials*. 2016;**30**:26-39
- [10] Pfannkuche JJ, Guo W, Cui S, Ma J, Lang G, Peroglio M, et al. Intervertebral disc organ culture for the investigation of disc pathology and regeneration - benefits, limitations, and future directions of bioreactors. *Connective Tissue Research*. 2019;**61**(3-4):1-18. DOI: 10.1080/03008207.2019.1665652
- [11] Endres S, Kratz M, Wunsch S, Jones DB. Zetos: A culture loading system for trabecular bone. Investigation of different loading signal intensities on bovine bone cylinders. *Journal of Musculoskeletal & Neuronal Interactions*. 2009;**9**(3):173-183
- [12] Jones DB, Boudriot U, Kratz M, Martens F, Koller K, Smith EL. A trabecular bone and marrow bioreactor. *European Cells & Materials*. 2001;**1**(suppl 2):53
- [13] Luo L, Thorpe SD, Buckley CT, Kelly DJ. The effects of dynamic compression on the development of cartilage grafts engineered using bone marrow and infrapatellar fat pad derived stem cells. *Biomedical Materials*. 2015;**10**(5):055011. DOI: 10.1088/1748-6041/10/5/055011

- [14] Raveling AR, Theodossiou SK, Schiele NR. A 3D printed mechanical bioreactor for investigating mechanobiology and soft tissue mechanics. *Methods*. 2018;**5**:924-932. DOI: 10.1016/j.mex.2018.08.001
- [15] Bourguine PE, Klein T, Paczulla AM, Shimizu T, Kunz L, Kokkaliaris KD, et al. In vitro biomimetic engineering of a human hematopoietic niche with functional properties. *Proceedings of the National Academy of Sciences of the United States of America*. 2018;**115**(25):E5688–E5695. DOI: 10.1073/pnas.1805440115
- [16] Gantenbein-Ritter B, Potier E, Zeiter S, van der Werf M, Sprecher CM, Ito K. Accuracy of three techniques to determine cell viability in 3D tissues or scaffolds. *Tissue Engineering. Part C, Methods*. 2008;**14**(4):353-358. DOI: 10.1089/ten.tec.2008.0313
- [17] Guggisberg S, Benneker LM, Keel MJ, Gantenbein B. Mechanical loading promoted Discogenic differentiation of human mesenchymal stem cells incorporated in 3D-PEG scaffolds with RhGDF5 and RGD. *International Journal of Stem cell Research & Therapy*. 2015;**2**(006):006. DOI: 10.23937/2469-570X/1410006
- [18] Frauchiger DA, Heeb SR, May RD, Wöltje M, Benneker LM, Gantenbein B. Differentiation of MSC and annulus fibrosus cells on genetically engineered silk fleece-membrane-composites enriched for GDF-6 or TGF- β 3. *Journal of Orthopaedic Research*. 2018;**36**(5):1324-1333. DOI: 10.1002/jor.23778
- [19] Gantenbein B, Frauchiger DA, May RD, Bakirci E, et al. Developing bioreactors to host joint-derived tissues that require mechanical stimulation. In: Reis RL, Gomes ME, editors. *Encyclopedia of Tissue Engineering and Regenerative Medicine*. 1st ed. NY: Elsevier; 2019. pp. 261-280
- [20] Martin I, Wendt D, Heberer M. The role of bioreactors in tissue engineering. *Trends in Biotechnology*. 2004;**22**(2):80-86. DOI: 10.1016/j.tibtech.2003.12.001
- [21] Wendt D, Jakob M, Martin I. Bioreactor-based engineering of osteochondral grafts: From model systems to tissue manufacturing. *Journal of Bioscience and Bioengineering*. 2005;**100**(5):489-494. DOI: 10.1263/jbb.100.489
- [22] Riss TL, Moravec RA, Niles AL, Duellman S, et al. Cell viability assays. In: Sittampalam GS, Grossman A, Brimacombe K, Arkin M, et al., editors. *Assay Guidance Manual*. Bethesda (MD): Eli Lilly & Company and the National Center for Advancing Translational Sciences; 2004. DOI: NBK144065 [bookaccession]
- [23] Bonnier F, Keating ME, Wróbel TP, Majzner K, Baranska M, Garcia-Munoz A, et al. Cell viability assessment using the alamar blue assay: A comparison of 2D and 3D cell culture models. *Toxicology In Vitro*. 2015;**29**(1):124-131. DOI: 10.1016/j.tiv.2014.09.014
- [24] Xiao J, Zhang Y, Wang J, Yu W, Wang W, Ma X. Monitoring of cell viability and proliferation in hydrogel-encapsulated system by resazurin assay. *Applied Biochemistry and Biotechnology*. 2010;**162**(7):1996-2007. DOI: 10.1007/s12010-010-8975-3
- [25] Plesca D, Mazumder S, Almasan A. Chapter 6 DNA damage response and apoptosis. *Methods in Enzymology*. 2008;**446**:107-122. DOI: 10.1016/S0076-6879(08)01606-6
- [26] Duchi S, Piccinini F, Pierini M, Bevilacqua A, Torre ML, Lucarelli E, et al. A new holistic 3D non-invasive analysis of cellular distribution and motility on fibroin-alginate microcarriers using light sheet

fluorescent microscopy. PLoS One. 2017;**12**(8):e0183336. DOI: 10.1371/journal.pone.0183336

[27] Rasband WS. ImageJ, USA, National Institutes of Health, Bethesda, Maryland, USA. 2020. Available from: <http://rsb.info.nih.gov/ij/> [Accessed: 22 May 2020]

[28] Bordbar S, Lotfi Bakhshaiesh N, Khanmohammadi M, Sayahpour FA, Alini M, Baghaban Eslaminejad M. Production and evaluation of decellularized extracellular matrix hydrogel for cartilage regeneration derived from knee cartilage. *Journal of Biomedical Materials Research. Part A.* 2020;**108**(4):938-946. DOI: 10.1002/jbm.a.36871

[29] Masson-Meyers DS, Bumah VV, Enwemeka CS. A comparison of four methods for determining viability in human dermal fibroblasts irradiated with blue light. *Journal of Pharmacological and Toxicological Methods.* 2016;**79**:15-22. DOI: 10.1016/j.vascn.2016.01.001

[30] Sanfilippo S, Canis M, Ouchchane L, Botchorishvili R, Artonne C, Janny L, et al. Viability assessment of fresh and frozen/thawed isolated human follicles: Reliability of two methods (trypan blue and calcein AM/ethidium homodimer-1). *Journal of Assisted Reproduction and Genetics.* 2011;**28**(12):1151-1156. DOI: 10.1007/s10815-011-9649-y

[31] Elson KM, Fox N, Tipper JL, Kirkham J, Hall RM, Fisher J, et al. Non-destructive monitoring of viability in an ex vivo organ culture model of osteochondral tissue. *European Cells & Materials.* 2015;**29**(0):356-369. DOI: 10.22203/eCM.v029a27

[32] Stoddart MJ, Furlong PI, Simpson A, Davies CM, Richards RG. A comparison of non-radioactive methods

for assessing viability in ex vivo cultured cancellous bone: Technical note. *European Cells & Materials.* 2006;**12**:16-25. Discussion 16-25. DOI: 10.22203/eCM.v012a02

[33] Rauch B, Edwards RB, Lu Y, Hao Z, Muir P, Markel MD. Comparison of techniques for determination of chondrocyte viability after thermal injury. *American Journal of Veterinary Research.* 2006;**67**(8):1280-1285. DOI: 10.2460/ajvr.67.8.1280

[34] Chang SW, Chou SF, Wang YH. Ethanol treatment induces significant cell death in porcine corneal fibroblasts. *Cornea.* 2006;**25**(9):1072-1079. DOI: 10.1097/01.icc.0000254200.69742.b5

[35] Catelas I, Sese N, Wu BM, Dunn JC, Helgerson S, Tawil B. Human mesenchymal stem cell proliferation and osteogenic differentiation in fibrin gels in vitro. *Tissue Engineering.* 2006;**12**(8):1-12. DOI: 10.1089/ten.2006.12.ft-97

[36] Haschtmann D, Stoyanov JV, Ettinger L, Nolte LP, Ferguson SJ. Establishment of a novel intervertebral disc/endplate culture model: Analysis of an ex vivo in vitro whole-organ rabbit culture system. *Spine.* 2006;**31**(25):2918-2925. DOI: 10.1097/01.brs.0000247954.69438.ae

[37] Melamed MR, Kamensky LA, Boyse EA. Cytotoxic test automation: A live-dead cell differential counter. *Science.* 1969;**163**(864):285-286. DOI: 10.1126/science.163.3864.285

[38] Supino R. MTT assays. *Methods in Molecular Biology.* 1995;**43**:137-149. DOI: 10.1385/0-89603-282-5:137

[39] Mosmann T. Rapid colorimetric assay for cellular growth and survival: Application to proliferation and cytotoxicity assays. *Journal of Immunological*

- Methods. 1983;**65**(1-2):55-63. DOI: 10.1016/0022-1759(83)90303-4
- [40] Oral HB, George AJ, Haskard DO. A sensitive fluorometric assay for determining hydrogen peroxide-mediated sublethal and lethal endothelial cell injury. *Endothelium*. 1998;**6**(2):143-151. DOI: 10.3109/10623329809072201
- [41] Lichtman JW. Confocal microscopy. *Scientific American*. 1994;**271**(2):40-45
- [42] Boyde A. Bibliography on confocal microscopy and its applications. *Scanning*. 1994;**16**:33-56
- [43] Gantenbein-Ritter B, Sprecher CM, Chan S, Illien-Jünger S, Grad S. Confocal imaging protocols for live/dead staining in three-dimensional carriers. *Methods in Molecular Biology*. 2011;**740**:127-140. DOI: 10.1007/978-1-61779-108-6_14
- [44] Perfetto SP, Chattopadhyay PK, Lamoreaux L, Nguyen R, Ambrozak D, Koup RA, et al. Amine reactive dyes: An effective tool to discriminate live and dead cells in polychromatic flow cytometry. *Journal of Immunological Methods*. 2006;**313**(1-2):199-208. DOI: 10.1016/j.jim.2006.04.007
- [45] Perfetto SP, Chattopadhyay PK, Lamoreaux L, Nguyen R, Ambrozak D, Koup RA, et al. Amine-reactive dyes for dead cell discrimination in fixed samples. *Current Protocols in Cytometry*. 2010;**Chapter 9**(July):1-14. DOI: 10.1002/0471142956.cy0934s53
- [46] Otsu N. A threshold selection method from gray-level histograms. *IEEE Transactions on Systems, Man, and Cybernetics*. 1979;**9**(1):62-66
- [47] Gantenbein B. Cell Viability Estimator for 3D Scaffolds for MATLAB. 2020. Available from: <https://www.mathworks.com/matlabcentral/fileexchange/75548-cell-viability-estimator-for-3d-scaffolds> [Accessed: 22 May 2020]
- [48] Chan SCW, Gantenbein-Ritter B, Leung VY, Chan D, Cheung KM, Ito K. Cryopreserved intervertebral disc with injected bone marrow-derived stromal cells: A feasibility study using organ culture. *The Spine Journal*. 2010;**10**(6):486-496. DOI: 10.1016/j.spinee.2009.12.019
- [49] Perez-Cruet M, Beeravolu N, McKee C, Brougham J, Khan I, Bakshi S, et al. Potential of human nucleus pulposus-like cells derived from umbilical cord to treat degenerative disc disease. *Neurosurgery*. 2019;**84**(1):272-283. DOI: 10.1093/neuros/nyy012
- [50] Wallace PK, Tario JD, Fisher JL, Wallace SS, Ernstoff MS, Muirhead KA. Tracking antigen-driven responses by flow cytometry: Monitoring proliferation by dye dilution. *Cytometry. Part A*. 2008;**73**(11):1019-1034. DOI: 10.1002/cyto.a.20619
- [51] Gertner-Dardenne J, Poupot M, Gray B, Fournié JJ. Lipophilic fluorochrome trackers of membrane transfers between immune cells. *Immunological Investigations*. 2007;**36**:5-6. DOI: 10.1080/08820130701674646
- [52] Yin X, Li P, Li Y, Cai Y, Wen J, Luan Q. Growth/differentiation factor-5 promotes in vitro/vivo periodontal specific differentiation of induced pluripotent stem cell-derived mesenchymal stem cells. *Experimental and Therapeutic Medicine*. 2017;**14**(5):4111-4117. DOI: 10.3892/etm.2017.5030
- [53] Yang Y, Mao Y, Wang J, Sun C, Zhang Y, Chen X. In vivo tracing of human amniotic mesenchymal stem cells labeled with PKH26 in rat intrauterine adhesions model. *Shengwu Gongcheng Xuebao/Chinese Journal of*

Biotechnology. 2018;**34**(10):1660-1667. DOI: 10.13345/j.cjb.180018

[54] Li P, Zhang R, Sun H, Chen L, Liu F, Yao C, et al. PKH26 can transfer to host cells in vitro and vivo. *Stem Cells and Development*. 2013;**22**(2):340-344. DOI: 10.1089/scd.2012.0357

[55] Ford JW, Welling TH, Stanley JC, Messina LM. PKH26 and 125I-PKH95: Characterization and efficacy as labels for in vitro and in vivo endothelial cell localization and tracking. *The Journal of Surgical Research*. 1996;**62**(1):23-28. DOI: 10.1006/jsre.1996.0167

[56] Dominkuš PD, Stenovec M, Sitar S, Lasič E, Zorec R, Plemenitaš A, et al. PKH26 labeling of extracellular vesicles: Characterization and cellular internalization of contaminating PKH26 nanoparticles. *Biochimica et Biophysica Acta - Biomembranes*. 2018;**1860**(6):1350-1361. DOI: 10.1016/j.bbmem.2018.03.013

[57] Sigma-Aldrich: PKH26 Red Fluorescent Cell Linker Kits for General Cell Membrane Labeling. Available from: <https://www.sigmaaldrich.com/content/dam/sigma-aldrich/docs/Sigma/Bulletin/pkh26glbul.pdf> [Accessed: 22 May 2020]

[58] Molecular Probes: Fisher Thermo Scientific, Inc. Vybrant Cell-Labeling Solutions. Available from: <http://www.icms.qmul.ac.uk/flowcytometry/uses/fret/diagrams/mp22885.pdf> [Accessed: 22 May 2020]

[59] Lehmann TP, Juzwa W, Filipiak K, Sujka-Kordowska P, Zabel M, Głowacki J, et al. Quantification of the asymmetric migration of the lipophilic dyes, DiO and DiD, in homotypic co-cultures of chondrosarcoma SW-1353 cells. *Molecular Medicine Reports*. 2016;**14**(5):4529-4536. DOI: 10.3892/mmr.2016.5793

[60] Nagyova M, Slovinska L, Blasko J, Grulova I, Kuricova M, Cigankova V, et al. A comparative study of PKH67, DiI, and BrdU labeling techniques for tracing rat mesenchymal stem cells. *In Vitro Cellular & Developmental Biology. Animal*. 2014;**50**(7):656-663. DOI: 10.1007/s11626-014-9750-5

[61] Frauchiger D, Tekari A, Benneker LM, Sakai D, Gantenbein B. Proceedings of the ORS. In: *The Fate of Allogeneic Injected Angiopoietin-1 Receptor Tie2+ Cells in Intervertebral Disc Organ Culture*. San Diego; 19-22 March, 2017

[62] Seiler C, Gazdhar A, Reyes M, Benneker LM, Geiser T, Siebenrock KA, et al. Time-lapse microscopy and classification of 2D human mesenchymal stem cells based on cell shape picks up myogenic from osteogenic and adipogenic differentiation. *Journal of Tissue Engineering and Regenerative Medicine*. 2014;**8**(9):737-746. DOI: 10.1002/term.1575

[63] Bertolo A, Gemperli A, Gruber M, Gantenbein B, Baur M, Pötzel T, et al. In vitro cell motility as a potential mesenchymal stem cell marker for multipotency. *Stem Cells Translational Medicine*. 2014;**4**(1):84-90. DOI: 10.5966/sctm.2014-0156

[64] Chan SC, Tekari A, Benneker LM, Heini PF, Gantenbein B. Osteogenic differentiation of bone marrow stromal cells is hindered by the presence of intervertebral disc cells. *Arthritis Research and Therapy*. 2015;**18**(1):29. DOI: 10.1186/s13075-015-0900-2

[65] Tekari A, May RD, Frauchiger DA, Chan SCW, Benneker LM, Gantenbein B. The BMP2 variant L51P restores the osteogenic differentiation of human mesenchymal stromal cells in the presence of intervertebral disc cells. *European Cells & Materials*. 2017;**33**:197-210. DOI: 10.22203/eCM.v033a15

- [66] Panebianco CJ, DiStefano TJ, Mui B, Hom WW, Iatridis JC. Crosslinker concentration controls TGF β -3 release and annulus fibrosus cell apoptosis in genipin-crosslinked fibrin hydrogels. *European Cells & Materials*. 2020;**39**: 211-226. DOI: 10.22203/eCM.v039a14
- [67] Frauchiger DA, May RD, Bakirci E, Tekari A, Chan SCW, Wöltje M, et al. Genipin-enhanced fibrin hydrogel and novel silk for intervertebral disc repair in a loaded bovine organ culture model. *Journal of Functional Biomaterials*. 2018;**9**(3):40. DOI: 10.3390/jfb9030040
- [68] Scheibler AG, Götschi T, Widmer J, Holenstein C, Steffen T, Camenzind RS, et al. Feasibility of the annulus fibrosus repair with in situ gelating hydrogels - A biomechanical study. *PLoS One*. 2018;**13**(12):e0208460. DOI: 10.1371/journal.pone.0208460
- [69] Liang HC, Chang WH, Lin KJ, Sung HW. Genipin-crosslinked gelatin microspheres as a drug carrier for intramuscular administration: in vitro and in vivo studies. *Journal of Biomedical Materials Research. Part A*. 2003;**65**(2):271-282. DOI: 10.1002/jbm.a.10476
- [70] Santos-Vizcaino E, Haley H, Gonzalez-Pujana A, Orive G, Hernandez RM, Luker GD, et al. Monitoring implantable immunoisolation devices with intrinsic fluorescence of genipin. *Journal of Biophotonics*. 2019;**12**(4):e201800170. DOI: 10.1002/jbio.201800170
- [71] Silva-Correia J, Gloria A, Oliveira MB, Mano JF, Oliveira JM, Ambrosio L, et al. Rheological and mechanical properties of acellular and cell-laden methacrylated gellan gum hydrogels. *Journal of Biomedical Materials Research. Part A*. 2013;**101**(12):3438-3446. DOI: 10.1002/jbm.a.34650
- [72] Silva-Correia J, Oliveira JM, Caridade SG, Oliveira JT, Sousa RA, Mano JF, et al. Gellan gum-based hydrogels for intervertebral disc tissue-engineering applications. *Journal of Tissue Engineering and Regenerative Medicine*. 2011;**5**(6):e97-e107. DOI: 10.1002/term.363
- [73] Frauchiger DA, Tekari A, May RD, Džafro E, Chan SC, Stoyanov J, et al. FACS is more potent to fish IVD progenitor cells than magnetic and bead-based methods. *Tissue Engineering. Part C, Methods*. 2019;**25**(10):571-580. DOI: 10.1089/ten.TEC.2018.0375
- [74] Lee JT, Cheung KM, Leung VY. Systematic study of cell isolation from bovine nucleus pulposus: Improving cell yield and experiment reliability. *Journal of Orthopaedic Research*. 2015;**33**(12):1743-1755. DOI: 10.1002/jor.22942
- [75] D'Arcy MS. Cell death: A review of the major forms of apoptosis, necrosis and autophagy. *Cell Biology International*. 2019;**43**(6):582-592. DOI: 10.1002/cbin.11137
- [76] Kanduc D, Mittelman A, Serpico R, Sinigaglia E, Sinha AA, Natale C, et al. Cell death: Apoptosis versus necrosis (review). *International Journal of Oncology*. 2002;**21**(1):165-170
- [77] Sellers JR, Cook S, Goldmacher VS. A cytotoxicity assay utilizing a fluorescent dye that determines accurate surviving fractions of cells. *Journal of Immunological Methods*. 1994;**172**(2):255-256. DOI: 10.1016/0022-1759(94)90112-0